A PARAMETRIC PILOT/CONTROL DEVICE MODEL FOR ROTORCRAFT BIODYNAMIC FEEDTHROUGH ANALYSIS

Pierangelo Masarati*, Giampiero Bindolino, Giuseppe Quaranta

Dipartimento di Scienze e Tecnologie Aerospaziali, Politecnico di Milano

via La Masa 34, 20156, Milano, Italy

{pierangelo.masarati,giampiero.bindolino,giuseppe.quaranta}@polimi.it

Abstract

This work presents a numerical model of the pilot/control device subsystem. The model is related to the left arm of a helicopter pilot holding a conventional collective control inceptor. A detailed biomechanical model of the pilot is developed within a general purpose multibody dynamics formulation. Linearized models about reference conditions are computed from the general analysis, for specific reference positions of the control inceptor and settings of the neuro-musculo-skeletal system that characterize specific flight conditions and tasks. The linearized models of the biodynamic feedthrough are used to produce coupled pilot/control device subsystem models that are parametrized with respect to the pilot biodynamic feedthrough characteristics and the mechanical properties of the control inceptor.

1. INTRODUCTION

The presence of the pilot in the control loop has several effects on the flight dynamics of aircraft. Through his cognitive action on the controls, the pilot determines the motion of the vehicle according to a mental model of the vehicle dynamics (feedforward), and compensates for discrepancies between the desired and the actual motion (feedback). The problem of adverse Aircraft-Pilot Couplings (APCs) surfaced from the very beginning of human flight, and received significant attention from the 1970s.[1] Focus has been mainly placed on the adverse effects of voluntary pilot action, called Pilot-Induced Oscillations (PIO), which are the consequence of a mismatch between the actual vehicle dynamics and the mental model the pilot uses to anticipate the control action.

Since control forces and moments are produced by the vehicle (in conventional helicopters, usually by means of the main and tail rotors) in response to actions on the control inceptors, the inadvertent or unintentional motion of the control inceptors may produce undesired control loads. This phenomenon is often caller Pilot-Augmented Oscillations (PAO). Those phenomena typically occur at frequencies that are too high to be effectively contrasted by the pilot's intentional action on the controls. In a research effort conducted in Europe within GARTEUR, HC AG-16,[2] the band of inter-est for aeroelastic RPCs has been conventionally set to 2 Hz to 8 Hz. Cockpit vibrations causing involuntary control action are filtered by the human limbs' biomechanics, which play a crucial role in the phenomenon called biodynamic feedthrough (BDFT).

Several studies have investigated the effects of fixed wing aircraft cockpit manipulators while performing compensatory tracking tasks (for example Magdaleno & McRuer[3] and McRuer & Magdaleno[4]). Subsequent works addressed the impact of vibration on pilot control, focusing on the feedthrough of vibration from the pilot to the control inceptors (for example Allen et al.,[5] and Jex & Magdaleno;[6] see also the review by McLeod & Griffin,[7] the work by Merhav & Idan[8] and that of Höhne[9]). The effects of lateral stick characteristics on pilot dynamics were further investigated from flight data by Mitchell et al.[10]

Adverse aeroelastic RPCs did not receive as much attention in the open literature as the fixed-wing (APC) counterpart, despite the evidence of occurrences since the 1960s. In 1968 Gabel and Wilson[11] discussed the problem of external sling load instabilities, considering the case of vertical bounce of the sling load interacting with the pilot through the collective control system. In 1992, Prouty and Yackle[12] discuss RPC as a possible cause of an accident that occurred during the troubled development of the AH-56 Cheyenne. In

2007, Walden[13] presented an extensive discussion of aeromechanical instabilities occurred to several rotorcraft during development and acceptance by the US Navy, including CH-46, UH-60, SH-60, CH-53, RAH-66, V-22 and AH-1. The history of tiltrotor development has seen several PAO events, from the early design and testing of the XV-15 technology demonstrator[14] to the aeroservoelastic pilot-in-the-loop couplings encountered during the development of the V-22.[13, 15] A complete database of PIO and PAO incidents occurred to rotary-wing aircraft is reported in.[1]

In the last decade, research efforts flourished in Europe; the coordinated activities of the already mentioned GARTEUR HC AG-16[2] and the ARISTOTEL 7th Framework Programme project[1][1, 16] deserve a mention, along with other activities (e.g.[17]).

The present work originates from an attempt to produce a detailed biomechanical model of the pilot's limbs involved in controlling a rotorcraft, to gain the capability to predict the BDFT characteristics of cockpit layouts and, specifically, to provide a tool for the tailoring of control inceptor dynamics. The objective is to give the designer the capability to include the pilot and control device dynamics in the analysis of the aeromechanics of the vehicle, to anticipate potential problems related to RPCs.

The work is organized as follows: the detailed biomechanical model of the left arm is presented; the identification of the BDFT transfer functions is discussed; the linearized pilot/control device model is presented; the linearized vehicle model is briefly presented, focusing on its integration with the pilot/control device model; selected results of stability sensitivity to pilot/control device parameters are discussed, followed by an example of control device tailoring to mitigate potentially adverse interaction.

2. APPROACH

2.1 Biodynamic Model of the Arm

Figure 1 presents the multibody model of a pilot's left arm holding a conventional collective control inceptor. The multibody model has been developed and presented in.[18–20]
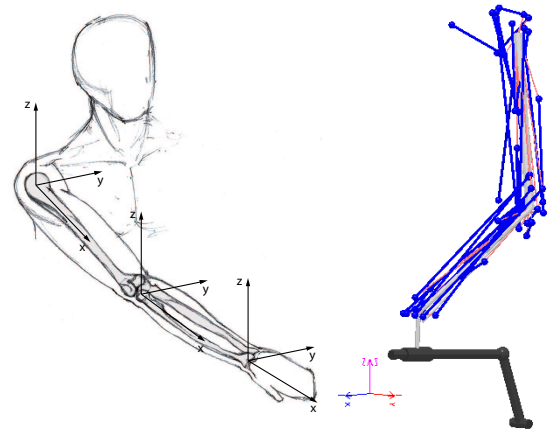
Figure 1: Multibody model of the arm holding the collective control inceptor.

(a) Block diagram

(b) Mechanical scheme
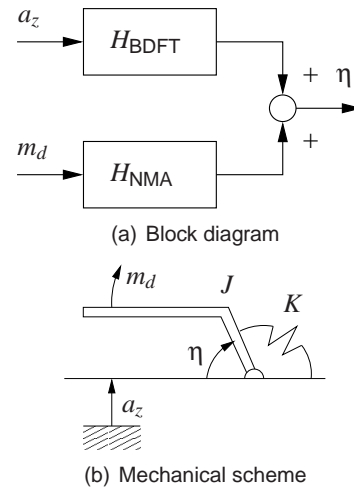
Figure 2: Block diagram and mechanical representation of feedthrough.

2.2 Transfer Function Identification

The involuntary motion of the control device, η, is expressed as a function of the platform motion, a_z, and of the moment applied to the control device, m_d, by means of the transfer functions $H_{\text{BDFT}}(s)$ and $H_{\text{NMA}}(s)$, namely

$$(1) \quad \eta = H_{\text{BDFT}}(s)a_z + H_{\text{NMA}}(s)m_d,$$

according to the block diagram of Fig. 2(a). The typical frequency response of functions $H_{\text{BDFT}}(s)$ and $H_{\text{NMA}}(s)$ is shown in Figs. 3, along with their fitting in terms of strictly proper transfer functions with the structure

$$(2) \quad H_{(\clubsuit)}(s) = \frac{b_{(\clubsuit)}}{s^2 + a_1 s + a_2},$$

(a) Biodynamic feedthrough (BDFT)   (b) Neuromuscular admittance (NMA)
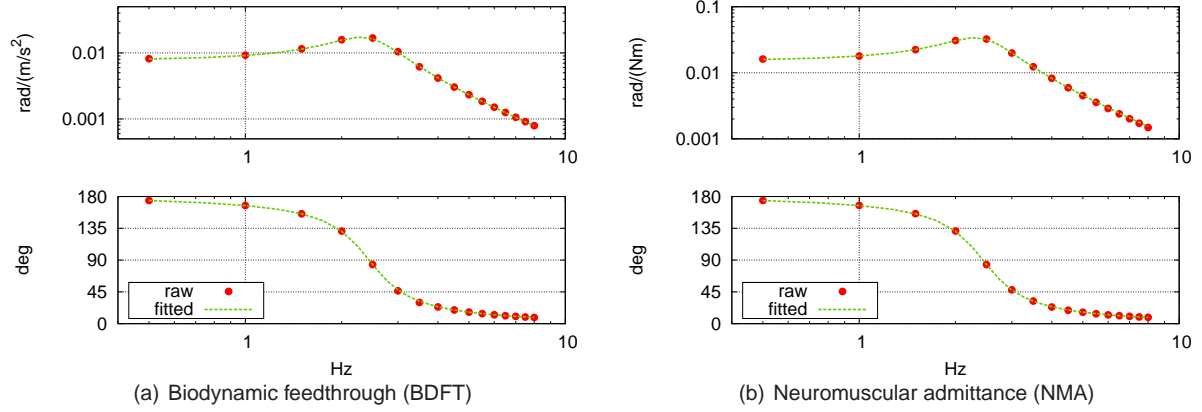
Figure 3: Fitting of numerical BDFT and NMA response with second-order transfer function (Eq. (2)).

with (♣) corresponding to BDFT and NMA. Equation (1) can be used to express the moment applied by the pilot to the control inceptor,

$$(3) \quad m_d = H_{\mathrm{NMA}}^{-1}(s)\left(\eta - H_{\mathrm{BDFT}}(s)a_z\right),$$

according to the scheme of Fig. 2(b).

2.3 Linearized Pilot/Control Device Model

The resulting equation of motion of the control device is thus

$$(4) \quad \left(J - \frac{1}{b_{\mathrm{NMA}}}\right)\ddot{\eta} + \left(C - \frac{a_1}{b_{\mathrm{NMA}}}\right)\dot{\eta} + \left(K - \frac{a_2}{b_{\mathrm{NMA}}}\right)\eta = m_e - \frac{b_{\mathrm{BDFT}}}{b_{\mathrm{NMA}}}a_z,$$

where J, C, and K are the mechanical parameters of the control device, whereas m_e is a generic external moment applied to the control device (e.g. friction,[21]). Eq. (4), in turn, can be added to a generic comprehensive or multibody rotorcraft aeromechanics analysis; alternatively, modified BDFT and NMA functions can be formulated, also accounting for the control device mechanical properties.

2.4 Linearized Vehicle Model

The helicopter dynamics is modeled using a state-space representation of the aeromechanics of a generic, medium weight helicopter representative of the Sud Aviation (now Airbus Helicopters) SA330. The model was initially presented in.[22] The linearized analysis is based on MASST,[23,24] a tool originally developed to integrate linearized

rotorcraft components. In the present case, a linearized aeroelastic model of the main rotor aeroelasticity, a structural dynamics model of the airframe, swashplate actuators dynamics models and an essential Stability and Control Augmentation System (SCAS) are combined to yield a state-space model of the helicopter trimmed in selected operating conditions. Hover and forward flight at 80 Kts are considered.

The linear state space model of the helicopter is described by the following equation,

$$(5) \quad \dot{\mathbf{x}}_h = \mathbf{A}_h\mathbf{x}_h + \mathbf{B}_h\mathbf{u}_h$$
$$(6) \quad \mathbf{y}_h = \mathbf{C}_h\mathbf{x}_h + \mathbf{D}_h\mathbf{u}_h.$$

The corresponding state-space representation of the approximated pilot/control device transfer function of Eq. (4) is

$$(7) \quad \dot{\mathbf{x}}_p = \mathbf{A}_p\mathbf{x}_p + \mathbf{B}_p\mathbf{u}_p$$
$$(8) \quad \mathbf{y}_p = \mathbf{C}_p\mathbf{x}_p,$$

with

(9) $\mathbf{x}_p = \left\{ \begin{array}{c} \eta \\ \dot{\eta} \end{array} \right\}$

(10)
$$\mathbf{u}_p = \left\{ \begin{array}{c} a_z \\ m_e \end{array} \right\}$$

(11)
$$\mathbf{y}_p = \eta$$

(12)
$$\mathbf{A}_p = \left[\begin{array}{cc} 0 & 1 \\ -\tilde{J}^{-1}\tilde{K} & -\tilde{J}^{-1}\tilde{C} \end{array} \right]$$

(13)
$$\mathbf{B}_p = \left[\begin{array}{cc} 0 & 0 \\ \tilde{J}^{-1}\tilde{\beta} & \tilde{J}^{-1} \end{array} \right]$$

(14)
$$\mathbf{C}_p = \left[\begin{array}{cc} 1 & 0 \end{array} \right];$$

the direct transmission term is $\mathbf{D}_p \equiv 0$, since the pilot/control device transfer function is strictly proper.

The coefficients in the pilot model are defined as

(15)
$$\tilde{J} = J - 1/b_{\mathrm{NMA}}$$

(16)
$$\tilde{C} = C - a_1/b_{\mathrm{NMA}}$$

(17)
$$\tilde{K} = K - a_2/b_{\mathrm{NMA}}$$

(18)
$$\tilde{\beta} = -b_{\mathrm{BDFT}}/b_{\mathrm{NMA}}$$

The coupled system dynamics is obtained by considering $\mathbf{u}_p = a_z = \mathbf{y}_h$ and $\mathbf{u}_h = \theta = G_c\eta = G_c\mathbf{y}_p$. The parameter G_c is the gearing ratio between the rotation of the control inceptor, η, and the main rotor blade pitch demand, θ. The coupled problem is thus

(19)
$$\left\{ \begin{array}{c} \dot{\mathbf{x}}_h \\ \dot{\mathbf{x}}_p \end{array} \right\} = \left[\begin{array}{cc} \mathbf{A}_h & \mathbf{B}_h G_c \mathbf{C}_p \\ \mathbf{B}_p \mathbf{C}_h & \left(\mathbf{A}_p + \mathbf{B}_p \mathbf{D}_h G_c \mathbf{C}_p\right) \end{array} \right] \left\{ \begin{array}{c} \mathbf{x}_h \\ \mathbf{x}_p \end{array} \right\}.$$

The measure of the vertical acceleration a_z at the pilot's seat is extracted from the vehicle model by defining an appropriate sensor.

The model of Eq. (19) is naturally parametrized in the gearing ratio G_c. Such parameter has a precise mechanical meaning; however, it also plays the role of a true feedback loop gain. A typical value for conventional helicopters, based on the cockpit layout considered in the analysis, is about 0.35 radian/radian (an end to end rotation of the control inceptor of about 45 deg corresponds to an end to end blade pitch rotation of 16 deg); pilots tend to prefer larger values, which means that the same amount of blade pitch rotation is achieved with smaller rotations of the inceptor, although intuitively increasing the feedback gain with respect to BDFT.

3. COUPLED MODEL ANALYSIS

This section puts the ingredients together to study the involuntary interaction between pilot and vehicle and its sensitivity with respect to the dynamic characteristics of the control device.

3.1 Parametric Stability Study

Figure 4 shows the eigenvalues of the coupled bioaeroservoelastic pilot-vehicle problem parametrized as a function of the gearing ratio G_c between the rotation of the control inceptor, η, and the collective pitch of the main rotor blades, $\theta = G_c\eta$, and the inertia, damping and stiffness of the control device.

The plots on the left and in the center give an overview of the distribution of the eigenvalues of the coupled model in the complex plane. The plots in Figs. 4 and 5 on the right show how the parameters influence some eigenvalues of the coupled system that are essential in the collective bounce phenomenon. Figure 4 refers to hover, whereas Fig. 5 refers to forward flight at 80 Kts. Collective bounce is a vertical oscillation of the helicopter that mainly involves the vertical displacement of the overall helicopter (the "heave" mode, indicated with H in the following), and the main rotor coning mode (MRC in the following), which is triggered by the pilot by acting on the collective control inceptor in involuntary response to the vertical acceleration of the vehicle.[25, 26]

The symbols ($\bigcirc$) indicate the sensitivity to the gearing ratio G_c, ranging from 0 radian/radian (darker symbols) to about 0.7 radian/radian (lighter ones) and nominal mechanical properties of the control device. At the reference value $G_c = 0.35$ radian/radian, the sensitivity to J, C, and K is evaluated. The figure shows that the pilot/control device mode (P/CD in the plot) moves to the left when the damping C is increased up to about 5 N·m·s/radian ($\triangle$), upwards when the stiffness K is increased up to 50 N·m/radian ($\square$), and downwards when the inertia increment ΔJ is increased up to 0.2 kg·m^2 (∇). In the two last cases, the damping factor of the coupled system slightly reduces.

At the same time, the damping of the main rotor coning mode increases when C grows, while it
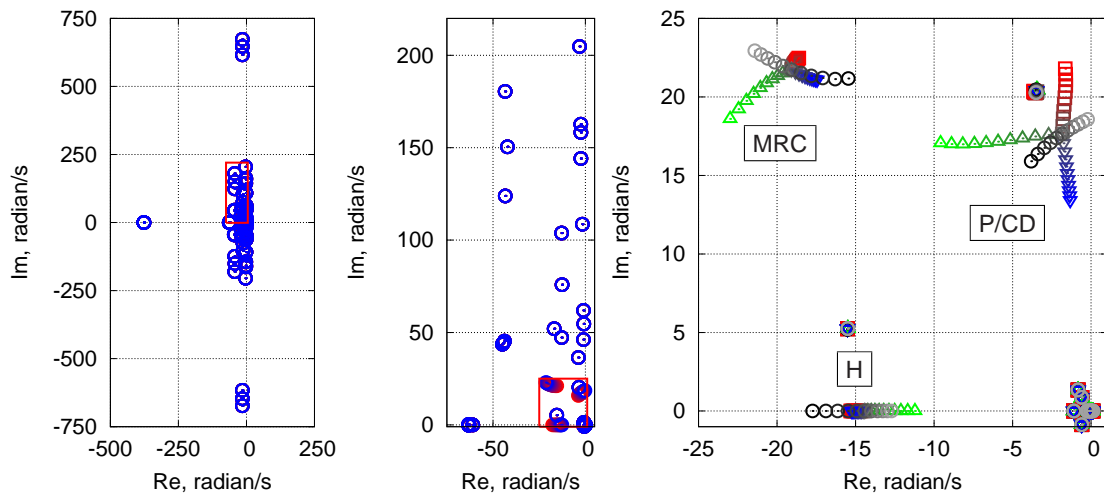
Figure 4: Coupled linearized model in hover; H: helicopter heave mode; MRC: main rotor coning mode; P/CD: pilot/control device mode; ◯: sensitivity to gearing ratio G_c; ▽: sensitivity to inertia ΔJ; △: sensitivity to damping C; □: sensitivity to stiffness K.
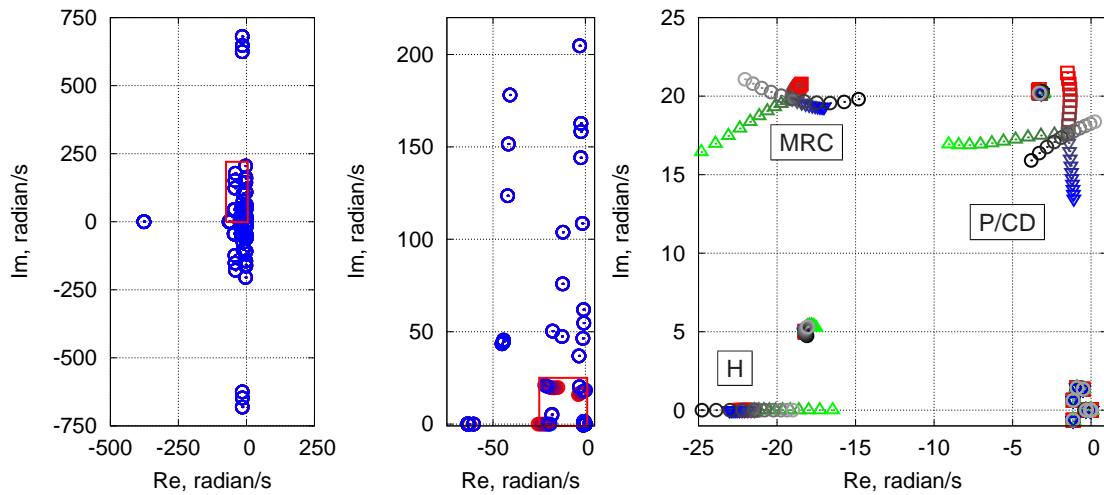
Figure 5: Coupled linearized model for $V_\infty = 80$ Kts; H: helicopter heave mode; MRC: main rotor coning mode; P/CD: pilot/control device mode; ◯: sensitivity to gearing ratio G_c; ▽: sensitivity to inertia ΔJ; △: sensitivity to damping C; □: sensitivity to stiffness K.
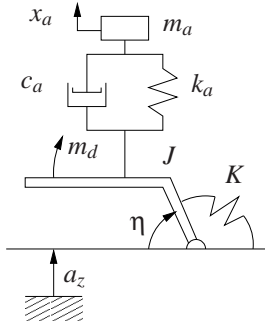
Figure 6: Sketch of collective control with dynamic absorber.

Figure 9: Pilot/control device impedance.

reduces when either J or K grow. On the contrary, the damping of the helicopter heave mode reduces when C grows and increases when either J or K grow.

The P/CD and MRC modes interact significantly. As G_c grows, The P/CD mode moves towards the right half-plane, approaching the imaginary axis for $G_c \approx 0.75$ (about twice the nominal value), whereas the MRC mode moves towards the left. The H mode also moves towards the right half-plane, although staying far away from instability.

3.2 Control Device Dynamics Tailoring

Having a simple but effective parametric model of the control device within a comprehensive aeromechanics analysis opens the possibility of very detailed and complex analysis. In this work, the addition of a tunable impedance device to the collective control inceptor is exploited as an example of possible means to improve the resilience of the coupled pilot-vehicle system to collective bounce and investigate the robustness of the proposed enhancement to uncertainties related to the biodynamics of the pilot.

Consider a simple dynamic absorber, consisting of a floating mass suspended at the control inceptor by means of a spring and a damper, as sketched in Fig. 6. The equation of motion of the dynamic absorber is

(20)
$$m_a \ddot{x}_a + c_a (\dot{x}_a - \ell \dot{\eta}) + k_a (x_a - \ell \eta) = 0,$$

where ℓ is a reference length that transforms the rotation of the inceptor, η, into the corresponding displacement of the dynamic absorber attachment point. The kinematics of an actual device could significantly differ from the sketch, and the sizing of the components (the mass m_a, the damper of characteristic c_a, and the spring of stiffness k_a) could be affected. However, the structure of Eq. (20) would not be affected.

Eq. (20) is added to the linearized coupled vehicle model by extending the state, in order to include x_a and $\dot{x}_a$, and by adding to the control device dynamics equation, Eq. (4), a contribution

(21)
$$m_e = \ell (c_a (\dot{x}_a - \ell \dot{\eta}) + k_a (x_a - \ell \eta)),$$

i.e. the moment produced by the force exchanged with the dynamic absorber by way of the connecting spring and damper.

Figure 7 illustrates the loop transfer function of the collective control with the involuntary pilot model in the loop, for unit G_c (recall that the baseline system is at the verge of stability for $G_c \approx 0.75$). The effect of the tunable impedance device in the loop can significantly modify the stability margins. In the specific case of the figure, for similar phase margin (in both cases $G_c \approx 0.5$ is needed for 60 deg phase margin, indicated with $\square$; the corresponding loop transfer functions are shown in Fig. 8); a significantly higher gain margin can be obtained ($G_{c_{\text{limit}}} \approx 1.35$ instead of $G_{c_{\text{limit}}} \approx 0.75$, indicated with $\bigcirc$, is needed to turn the system unstable).

Figure 9 illustrates the mechanical impedance of the pilot/control device system in the nominal case, with extra damping in $\tilde{C}$, and with the dynamic absorber. One can appreciate how the addition of a pure damping may significantly increase the amount of torque that needs to be applied to rotate the inceptor in the vicinity of the natural frequency of the pilot/control device system, from less than 1 Hz to and above 5 Hz, thus also affecting the upper bound of the band of interest of the voluntary action. On the contrary, the addition of the tunable device produces a smaller increase in re-

(a) Bode plot.

(b) Nyquist plot.
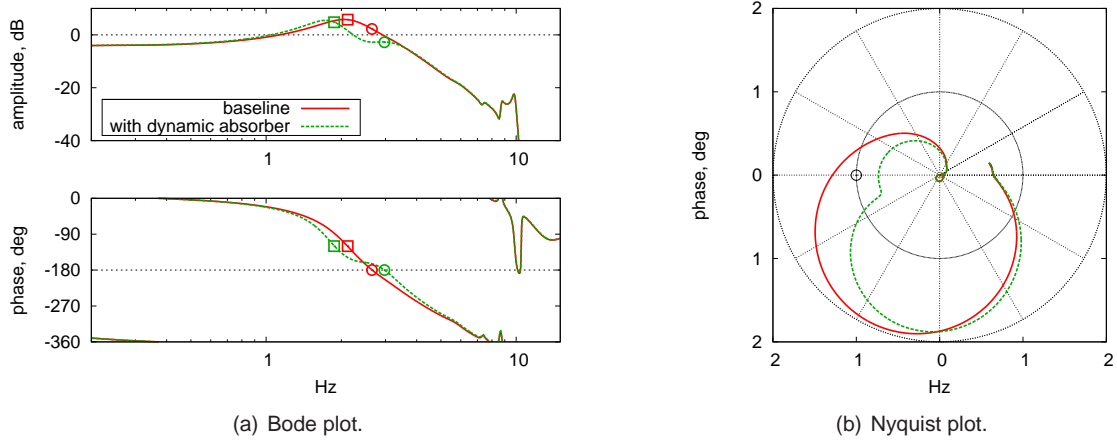
Figure 7: Collective control loop transfer function with parametric involuntary pilot model and unit G_c, in baseline and with tunable impedance device (dynamic absorber; □: phase margin, ○: gain margin).

(a) Bode plot.

(b) Nyquist plot.
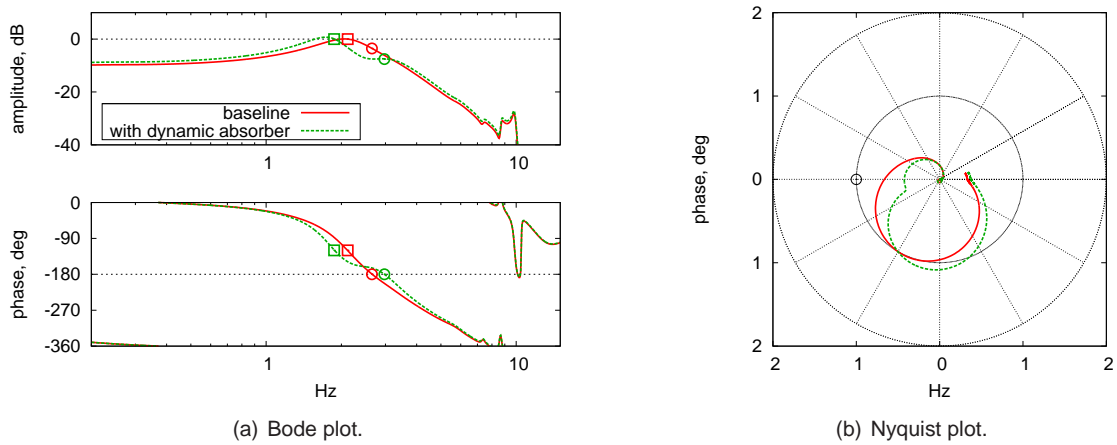
Figure 8: Collective control loop transfer function with parametric involuntary pilot model and 60 deg phase margin, in baseline and with tunable impedance device (dynamic absorber; □: phase margin, ○: gain margin).

quired torque, which is concentrated in the 2 Hz to 3 Hz band.

4. CONCLUSIONS

This work presented a linearized pilot/control device model of a conventional helicopter collective control inceptor. The transfer function of the pilot biomechanics is obtained from a detailed multibody analysis of the biomechanics of a human arm. Such data can be thus produced also for arbitrary cockpit configurations, without the need to perform dedicated tests. The pilot/control device model is coupled to a linearized aeroservoelastic model of a helicopter, to illustrate how it can be used to perform parametric analyses of the influence of control device dynamics on the aeroelastic stability of the coupled system. Furthermore, the coupled model is used to investigate the possibility to further tailor the dynamics of the coupled system by augmenting the control inceptor with passive tunable impedance devices. A simple dynamic absorber is added to the control inceptor and tuned to increase the stability margins of the coupled system.

References

[1] Marilena D. Pavel, Michael Jump, Binh Dang-Vu, Pierangelo Masarati, Massimo Gennaretti, Achim Ionita, Larisa Zaichik, Hafid Smaili, Giuseppe Quaranta, Deniz Yilmaz, Michael Jones, Jacopo Serafini, and Jacek Malecki. Adverse rotorcraft pilot couplings — past, present and future challenges. *Progress in Aerospace Sciences*, 62:1–51, October 2013. doi:10.1016/j.paerosci.2013.04.003.

[2] O. Dieterich, J. Götz, B. DangVu, H. Haverdings, P. Masarati, M. D. Pavel, M. Jump, and M. Gennaretti. Adverse rotorcraft-pilot coupling: Recent research activities in Europe. In *34th European Rotorcraft Forum*, Liverpool, UK, September 16–19 2008.

[3] R. E. Magdaleno and D. T. McRuer. Effects of manipulator restraints on human operator performance. AFFDL TR-66-72, 1966.

[4] D. T. McRuer and R. E. Magdaleno. Human pilot dynamics with various manipulators. AFFDL-TR 66-138, 1966.

[5] R. Wade Allen, Henry R. Jex, and Raymond E. Magdaleno. Manual control performance and dynamic response during sinusoidal vibration. AMRL-TR 73-78, October 1973.

[6] Henry R. Jex and Raymond E. Magdaleno. Biomechanical models for vibration feedthrough to hands and head for a semisupine pilot. *Aviation, Space, and Environmental Medicine*, 49(1–2):304–316, 1978.

[7] R. W. McLeod and M. J. Griffin. Review of the effects of translational whole-body vibration on continuous manual control performance. *Journal of Sound and Vibration*, 133(1):55–115, 1989. doi:10.1016/0022-460X(89)90985-1.

[8] S. J. Merhav and M. Idan. Effects of biodynamic coupling on the human operator model. *J. of Guidance, Control, and Dynamics*, 13(4):630–637, 1990. doi:10.2514/3.25380.

[9] Gordon Höhne. Computer aided development of biomechanical pilot models. *Aerospace Science and Technology*, 4(1):57–69, January 2000. doi:10.1016/S1270-9638(00)00117-6.

[10] David G. Mitchell, Bimal L. Aponso, and David H. Klyde. Effects of cockpit lateral stick characteristics on handling qualities and pilot dynamics. CR 4443, NASA, 1992.

[11] Richard Gabel and Gregory J. Wilson. Test approaches to external sling load instabilities. *Journal of the American Helicopter Society*, 13(3):44–55, 1968. doi:10.4050/JAHS.13.44.

[12] Ray W. Prouty and Al R. Yackle. The Lockheed AH-56 Cheyenne — Lessons learned. In *AIAA Aircraft Design Systems Meeting*, Hilton Head, SC, USA, August 24–26 1992. AIAA-1992-4278.

[13] R. Barry Walden. A retrospective survey of pilot-structural coupling instabilities in naval rotorcraft. In *American Helicopter Society 63rd Annual Forum*, pages 1783–1800, Virginia Beach, VA, May 1–3 2007.

[14] J.M. Bilger, R.L. Marr, and A. Zahedi. Results of structural dynamic testing of the XV-15 tilt rotor research aircraft. *Journal of the American Helicopter Society*, 27(2):58–65, 1982.

[15] T. Parham, Jr., David Popelka, David G. Miller, and Arnold T. Froebel. V-22 pilot-in-the-loop aeroelastic stability analysis. In *American Helicopter Society 47th Annual Forum*, Phoenix, Arizona (USA), May 6–8 1991.

[16] Marilena D. Pavel, Jacek Malecki, Binh DangVu, Pierangelo Masarati, Massimo Gennaretti, Michael Jump, Hafid Smaili, Achim Ionita, and Larisa Zaicek. A retrospective survey of adverse rotorcraft pilot couplings in European perspective. In *American Helicopter Society 68th Annual Forum*, Fort Worth, Texas, May 1–3 2012.

[17] Valeria Mariano, Giorgio Guglieri, and Andrea Ragazzi. Application of pilot induced oscillations prediction criteria to rotorcraft. In *American Helicopter Society 67th Annual Forum*, Virginia Beach, VA, May 3–5 2011.

[18] Pierangelo Masarati, Giuseppe Quaranta, and Andrea Zanoni. Dependence of helicopter pilots' biodynamic feedthrough on upper limbs' muscular activation patterns. *Proc. IMechE Part K: J. Multibody Dynamics*, 227(4):344–362, December 2013. doi:10.1177/1464419313490680.

[19] Pierangelo Masarati and Giuseppe Quaranta. Coupled bioaeroservoelastic rotorcraft-pilot simulation. In *Proceedings of ASME IDETC/CIE*, Portland, OR, August 4–7 2013. DETC2013-12035.

[20] Pierangelo Masarati and Giuseppe Quaranta. Bioaeroservoelastic analysis of involuntary rotorcraft-pilot interaction. *J. of Computational and Nonlinear Dynamics*, 9(3):031009, July 2014. doi:10.1115/1.4025354.

[21] Stefano Zanlucchi, Pierangelo Masarati, and Giuseppe Quaranta. A pilot-control device model for helicopter sensitivity to collective bounce. In *ASME IDETC/CIE 2014*, Buffalo, NY, August 17–20 2014. DETC2014-34479.

[22] Vincenzo Muscarello, Pierangelo Masarati, and Giuseppe Quaranta. Multibody analysis of rotorcraft-pilot coupling. In P. Eberhard and P. Ziegler, editors, *2nd Joint International Conference on Multibody System Dynamics*, Stuttgart, Germany, May 29–June 1 2012.

[23] Pierangelo Masarati, Vincenzo Muscarello, and Giuseppe Quaranta. Linearized aeroservoelastic analysis of rotary-wing aircraft. In *36th European Rotorcraft Forum*, pages 099.1–10, Paris, France, September 7–9 2010.

[24] Pierangelo Masarati, Vincenzo Muscarello, Giuseppe Quaranta, Alessandro Locatelli, Daniele Mangone, Luca Riviello, and Luca Viganò. An integrated environment for helicopter aeroservoelastic analysis: the ground resonance case. In *37th European Rotorcraft Forum*, pages 177.1–12, Gallarate, Italy, September 13–15 2011.

[25] Massimo Gennaretti, Jacopo Serafini, Pierangelo Masarati, and Giuseppe Quaranta. Effects of biodynamic feedthrough in rotorcraft-pilot coupling: Collective bounce case. *J. of Guidance, Control, and Dynamics*, 36(6):1709–1721, 2013. doi:10.2514/1.61355.

[26] Vincenzo Muscarello, Giuseppe Quaranta, and Pierangelo Masarati. The role of rotor coning in helicopter proneness to collective bounce. *Aerospace Science and Technology*, 36:103–113, July 2014. doi:10.1016/j.ast.2014.04.006.

COPYRIGHT STATEMENT